

Synthesis of ZnO nanoparticles and its application in adsorption

Karuna Nalwa, Anupama Thakur*, Neeta Sharma*

Dr SSBUI CET, Panjab University, Chandigarh, 160014, India

*Corresponding author: Tel: (+91)- 9356690680; E-mail: anupamat@pu.ac.in, neeta94@ymail.com

Received: 31 March 2016, Revised: 30 September 2016 and Accepted: 19 April 2017

DOI: 10.5185/amp/2017/696

www.vbripress.com/amp

Abstract

In the present study nanoparticles of zinc oxide (ZnO) were synthesized by simple solution based approach and used as an adsorbent for the removal of Cu(II) ions from aqueous solution. ZnO nanoparticles were characterized by X-Ray Diffraction (XRD), Transmission Electron Microscopy (TEM) and Dynamic Light Scattering (DLS). TEM confirmed the formation of zinc oxide nanoparticles in the size range of 10-11 nm. Adsorption capacity of ZnO for removing Cu(II) ions from aqueous solutions was investigated at different pH, as a function of contact time, metal ion concentration and the amount of adsorbent. Moreover, adsorption isotherms and kinetics was studied to understand the nature and mechanism of adsorption. A high percentage removal (98.71%) of Cu(II) from its aqueous solutions at pH 5 and at initial heavy metal ion concentration of 300 mg/l by ZnO particles was achieved. The adsorption isotherm was well described by Freundlich isotherm model ($R^2 = 0.999$). The adsorption kinetics data was well fitted by the pseudo-second-order rate model with a high regression coefficient. The above results suggest that ZnO nanoparticles can be used as potential adsorbent for the efficient removal of heavy metals from aqueous solutions. Copyright © 2017 VBRI Press.

Keywords: Zinc oxide nanoparticles, Cu(II) ions, adsorption, isotherm, kinetics.

Introduction

Pollution of water bodies by heavy metals released into the environment from metal plating industry, mining operations, welding and alloy manufacturing units is a matter of grave concern [1]. Water being the life support for humans and animals alike, its contamination by heavy metal ions poses severe health problems as they bind to proteins, nucleic acids and small metabolites causing either the alteration or loss of biological function [2]. Treatment of industrial waste water which frequently contains high levels of heavy metals is therefore required before the disposal in order to avoid water pollution. Copper is an essential trace nutrient to all high plants and animals including humans; however, if present in sufficient amounts can prove to be poisonous and even fatal. According to World Health Organization (WHO) standards, the maximum allowable concentration of copper in drinking water is 2 mg/l [3]. Several methods, including chemical precipitation, ion exchange, liquid-liquid extraction, electrodialysis and resins have been developed for the removal of heavy metal ions from industrial wastewater. Each method has its limitations in terms of cost, complexity or efficiency. Adsorption on the other hand is recognized as an effective and economic method. In recent years, nanoparticles have received significant attention due to their novel properties and have

come up as an area of extensive research in their utilization as adsorbents [4-7]. Nanoparticles have high surface area to volume ratio, thus offering larger number of active sites for the interaction of pollutant species for increased adsorption capacity. Although adsorption studies of heavy metal ions on metal oxide nanoparticles have been reported before, relatively few studies have been investigated on the removal of Cu(II) ions by ZnO nanoparticles [8].

The objective of the present study was to synthesize ZnO nanoparticles using a simple solution-based approach and its use as a possible alternative to low cost adsorbents for the removal of heavy metal ions from aqueous solutions. The ZnO nanoparticles were successfully synthesized and characterized by various analytical techniques. The effects of initial metal ion concentration, contact time, pH and amount of adsorbent on adsorption capacity of ZnO have been investigated. The synthesized ZnO nanoparticles exhibited high removal efficiency (~ 98.71%) of Cu(II) ions from its aqueous solutions.

Therefore, based on the above mentioned advantages of ease of preparation, reasonable cost and high removal efficiency, the synthesized nanoparticles suggest a potential application as an adsorbent in the removal of heavy metals from aqueous solutions.

Experimental

Materials

Zinc sulfate ($\text{ZnSO}_4 \cdot 7\text{H}_2\text{O}$) and Copper sulfate ($\text{CuSO}_4 \cdot 5\text{H}_2\text{O}$) were supplied by S.D. Fine Chemicals Ltd.(India); Sodium hydroxide pellets, liquor ammonia and Hydrochloric acid (HCl) were obtained from Merck (India). All the chemicals and reagents used were of analytical grade. All the solutions were prepared in double distilled water.

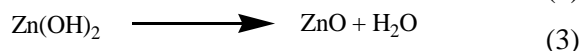
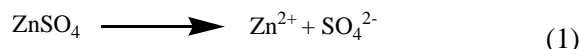
Method

Preparation of adsorbate solution

Copper sulfate stock solution (300 mg/l) was prepared by dissolving 1.178 g $\text{CuSO}_4 \cdot 5\text{H}_2\text{O}$ in 1 litre distilled water. For further experiments, the stock solution of Cu(II) was diluted to obtain working solutions of varying concentrations, *i.e.* 30 mg/l to 300 mg/l. 0.1M NaOH and 0.1M HCl were used for the adjustment of the pH (ranges from 2 to 5).

Preparation of ZnO nanoparticles

0.2M solution of zinc sulfate was prepared by dissolving 5.7508 g of $\text{ZnSO}_4 \cdot 7\text{H}_2\text{O}$ in 100 ml distilled water. 25 ml of this solution diluted with 50 ml of distilled water was used for experiment (mother solution). 4M solution of sodium hydroxide was prepared by dissolving 16 g of NaOH pellets in 100 ml distilled water. Then 25 ml of the alkali solution was added at an approximate rate of 5 ml/min to the mother solution, under continuous stirring. The pH of the mixture was fixed at 13 as highly basic conditions are conducive to the direct preparation of ZnO nanoparticles [9]. The mixture was maintained at 60°C and precipitation occurred about 2h after mixing the solutions. The supernatant was decanted and the product was washed with distilled water. The product was centrifuged and washed with deionized water and finally dried at 60°C in hot air oven. The formation of ZnO takes place according to the following reactions (1-3) [9]:



Characterization of ZnO nanoparticles

The structural properties of synthesized sample were investigated using powder X-ray diffraction (XRD), (XPRT-PRO diffractometer) with $\text{Cu K}\alpha$ radiation ($\lambda = 0.1542 \text{ nm}$) operating at a voltage of 45 kV and a current of 40 mA. The scanning was done in the 2θ range from 10° to 80° with a step size of 0.017° and scan step time of 20.03s. Transmission electron microscopy (TEM) characterization was done using Hitachi H-7500 (Tokyo, Japan) operating at 100 kV. Dynamic light scattering (DLS) (Horiba instrument SZ-100) was used to determine the hydrodynamic size.

Colorimetric determination of copper

The spectrophotometric method of analysis was used for the measurement of copper content in solutions. The determination of copper is dependent upon the production of the intense blue color of the cupric ammonia complex when ammonia is added to the solution of a cupric salt. To produce the color system, 1 ml of 3M ammonium hydroxide was added to 10 ml of the standard copper solution, and thoroughly shaken [10]. The absorbance was measured against a corresponding blank solution. The same concentration of ammonium hydroxide was used in making unknown as well as standard solutions. The copper content in an unknown sample was determined from the calibration graph obtained at the various pH values of the solution under study.

Adsorption experiments

Batch mode was used to evaluate the parameters that influence the process of adsorption of Cu(II) ions on ZnO nanoparticles. Adsorption of Cu(II) was studied using aqueous solutions of copper sulfate with concentration ranging between 30 mg/l to 300 mg/l. In this method, a fixed amount of ZnO nanoparticles (100 mg) was added to a known volume of metal ion solution (10 ml), with its pH adjusted (in the range 2 to 5). pH of the solution was adjusted using dilute HCl or NaOH as per requirement. Studies beyond pH 5 have not been undertaken as metal hydroxide precipitation occurs. The test tubes were subjected to agitation. The solutions were centrifuged at varying intervals of time and the supernatant liquids were estimated for the final (residual) concentrations of Cu(II) ions using UV-visible Spectrophotometer. The percentage removal was calculated according to eq.(4):

$$\% \text{removal} = \left(\frac{C_o - C_e}{C_o} \right) \times 100 \quad (4)$$

where C_o and C_e are the initial and final concentrations of heavy metal ion in the solution phase (mg l^{-1}).

Results and discussion

Characterization of ZnO nanoparticles

Fig. 1 illustrates the XRD pattern of ZnO nanoparticles. XRD analysis indicates that the prepared ZnO nanoparticles are pure zinc oxide (JCPDS card 36-1451) and lie in the nanoscale range. Major diffraction peaks are seen at 31.73 , 34.39 , 36.24 , 47.51 , 56.52 , 62.88 , 67.94 , 72.54 and 76.89 , which can be assigned to diffraction from (100), (002), (101), (102), (110) and (103) planes, respectively [11].

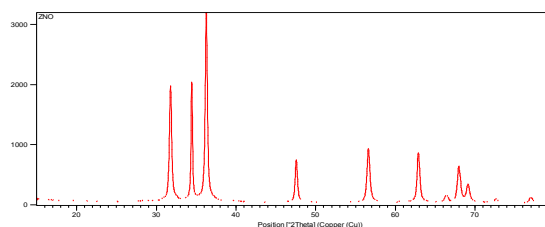


Fig. 1. XRD pattern of ZnO nanoparticles.

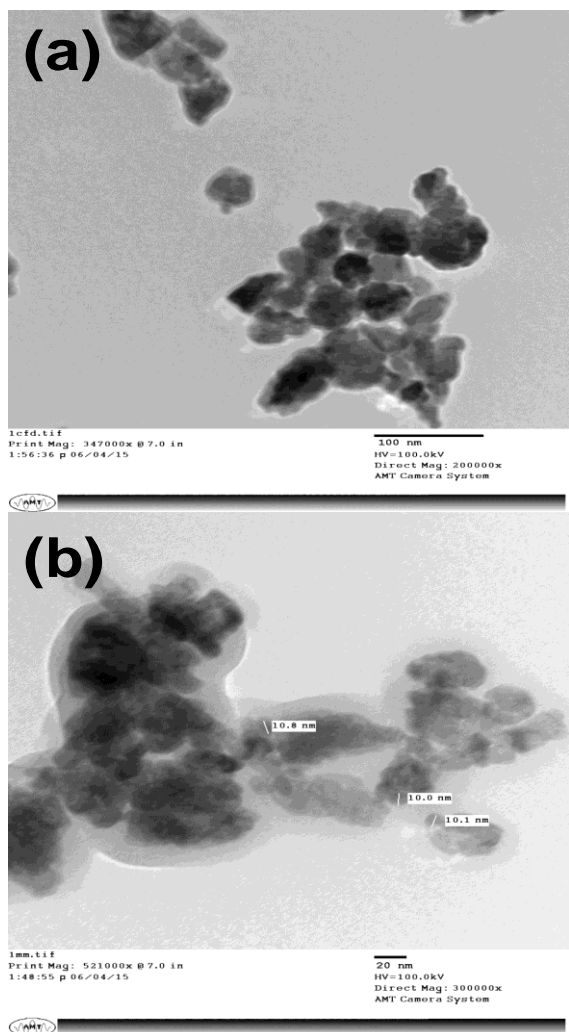


Fig. 2. (a, b) TEM images of ZnO nanoparticles at different magnification.

The strong and narrow diffraction peaks indicate that the product has good crystallinity. The synthesized nanopowder is free of impurities as it does not contain any characteristic XRD peaks other than ZnO peaks. The diameter of the synthesized ZnO nanoparticles has been calculated using the well-known Debye-Scherrer equation [11]:

$$d = \frac{0.89\lambda}{\beta \cos\theta} \tag{5}$$

where, 0.89 is Scherrer’s constant, λ is the X-ray wave length equal to 1.54 Å, β is the full width at half maximum and θ is half the diffraction angle. The average particle size of the sample as calculated using eq.(5) was found to be 68.61 nm, which was derived from the FWHM (0.2676) of more intense peak corresponding to (101) plane located at 36.24°. TEM images of synthesized zinc oxide nanoparticles are depicted in Fig. 2(a,b) at two different magnifications. From the images, it can be seen that the particles have dimensions ranging from 10 nm to

11 nm. Dynamic light scattering was used to determine the hydrodynamic size of zinc oxide nanoparticles and Fig. 3 shows the Z-average hydrodynamic diameter as 106.6 nm and polydispersity index (PI) as 0.296.

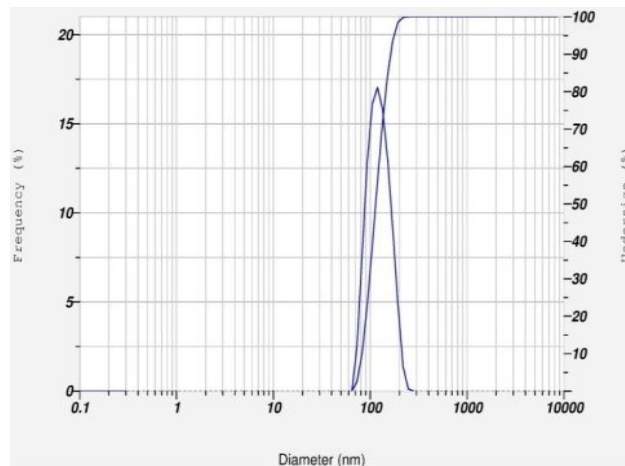


Fig. 3. Size distribution of zinc oxide nanoparticles using DLS.

Spectrophotometric determination of copper

The estimation of Cu(II) has been carried out spectrophotometrically by studying the absorption spectra of the copper(II)-ammonia system using a UV-visible spectrophotometer. The absorption spectrum is a symmetric curve with the maximum absorbance λ_{max} at 605 nm for pH 2. In all instances for pH 2, measurements were made at 605 nm against a reference. The absorption spectra was recorded for each pH studied (pH 2 to 5) and measurements taken at λ_{max} characteristic to each pH. The calibration curves have been plotted at different pH values of the solution for the concentration range under study i.e. 30-300 mg/l. Beer Lambert’s law is followed in all the cases.

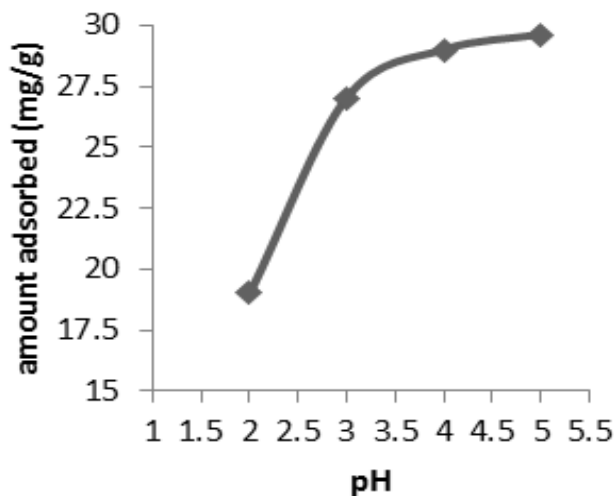


Fig. 4. Effect of solution pH on amount of Cu(II) adsorbed on ZnO nanoparticles. Condition: initial concentration 300 mg/l, time 90 min, amount of adsorbent 100mg.

Adsorption studies

Effect of pH

The pH value plays a very important role in the adsorption of copper ions on ZnO nanoparticles. It is a commonly known fact that anions are favorably adsorbed by the adsorbent at lower pH values due to presence of H^+ ions and cations are adsorbed at high pH values due to negatively charged ions. The effect of pH on the adsorption of Cu(II) ions for initial metal ion concentration of 300 mg/l, was studied in the pH range 2-5 (higher pH could not be studied as precipitation of metal ions occurs) and the results are shown in Fig. 4. It was observed that the adsorption of metal ions increased with increase in the solution pH. The effect of solution pH on adsorption can be explained on the basis of surface charge of the ZnO [12,13].



At a lower pH, the oxide surface will have positive character and there exists a competition between H^+ ions and highly competitive Cu(II) ions in solution for the active surface sites. The binding sites at adsorbent at low pH are dominated by the H^+ ions leading to protonated functional groups which inhibit the adsorption of metal ions over it. The adsorption of metal ions increased with increase of pH of the solution due to increasing electrostatic force of attraction between positively charged sorbate and negatively charged sorbent. The maximum removal was observed at pH 5. With an increase of pH from 2 to 5, the uptake of Cu(II) ions on ZnO increased from 63.4% to 98.71%.

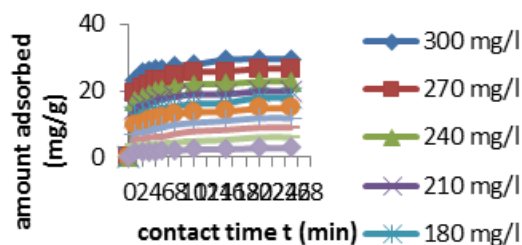


Fig. 5. Amount of Cu(II) adsorbed (mg/g) versus contact time t (min) on ZnO nanoparticles at different initial metal ion concentrations at pH-5.

Effect of initial metal ion concentration

The uptake of metal ion was observed to increase with increase in initial metal ion concentration in the range of concentrations studied, i.e. 30 mg/l to 300 mg/l. The dependence of adsorption capacity of ZnO nanoparticles on the initial metal ion concentration of Cu(II) is shown in Fig. 5. The adsorption at different concentrations was rapid during the initial stages, which gradually decreased with the progress of adsorption until the equilibrium was reached. This increase in the adsorption is a result of the increase in driving force due to concentration gradient

developed between the bulk solution and surface of the nanoparticles. At higher concentrations of metal ions, the driving force is higher and as the active sites of ZnO nanoparticles were surrounded by much more metal ions, the process of adsorption continues leading to an increased uptake of metal ions from the solution [12]. Therefore, the values of adsorption capacity increased with the increase of initial metal ion concentrations. The maximum adsorption took place when the initial metal ion concentration was maximum i.e. 300 mg/l.

Effect of contact time

The relation between contact time and adsorption of heavy metal ions on ZnO nanoparticles is shown in Fig. 5. It can be clearly seen from the figure that the amount adsorbed increases with increase in the contact time till equilibrium was attained. For adsorption studied at pH 2, the time to reach equilibrium was about 90 minutes whereas equilibrium was attained much more rapidly (within 20 minutes) for pH 3, 4 & 5. The initial faster adsorption rate of Cu(II) ions was due to the availability of a larger number of active adsorption sites during the initial period of contact and thereafter the adsorption is slow. In the adsorption process, initially the Cu(II) ions encountered boundary layer effect and then diffused from boundary layer to surface of metal oxides, finally they diffused into porous structure, therefore higher concentration solution takes relatively longer time to reach equilibrium.

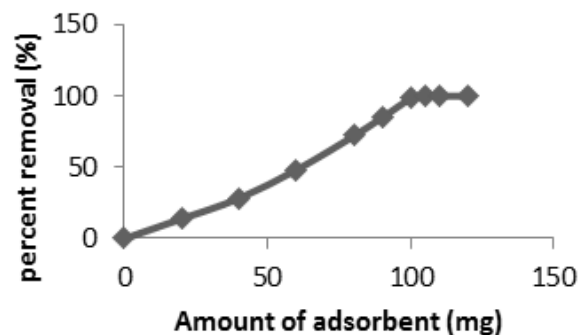


Fig. 6. Effect on amount of adsorbent on percent removal of Cu(II). Condition: initial concentration 300 mg/l, time 20 min, pH-5.

Effect of adsorbent dose

The effect of amount of ZnO nanoparticles on the adsorption of Cu(II) ions (Fig. 6) from their aqueous solutions was examined by varying the amount of adsorbent from 20 to 120 mg per 10 ml at pH 5 for a contact time of 20 min. With increase in the amount of adsorbent, percentage removal of Cu(II) ions was found to increase. The rapid increase in adsorption with the increase in adsorbent dose can be attributed to increased availability of binding sites resulting from the increased dose and conglomeration of the adsorbent. It was observed that Cu(II) removal efficiency increased with increasing adsorbent dose, up to 105 mg after which it

became almost constant. After the critical dose, the extent of adsorption slows down due to the fact that although there is increasing number of binding sites but there is shortage of adsorbate in the solution.

Adsorption isotherm modeling

Adsorption data has been subjected to Langmuir and Freundlich models as they are the most common isotherms describing solid-liquid adsorption system. Isotherms are the equilibrium relations between the concentration of adsorbate on the solid phase and its concentration in the liquid phase and from these isotherms the maximum adsorption capacity can be obtained. The adsorption studies were conducted at conditions of initial metal ion concentration 300 mg l^{-1} , contact time 20 min and solution pH 5 for adsorption of Cu(II) ions on zinc oxide nanoparticles.

Langmuir-isotherm model

Langmuir isotherm is often used to describe adsorption of solute from liquid solutions and this model assumes monolayer adsorption onto a homogeneous surface with finite number of identical sites and expressed by the following equation [14]:

$$\frac{C_e}{Q_e} = \frac{1}{Q_0 b} + \frac{C_e}{Q_e} \quad (9)$$

where, C_e is the final (residual) concentration (mg l^{-1}), Q_e is the amount of metal uptake at equilibrium (mg g^{-1}) and Q_0 (mg g^{-1}) and b (mg^{-1}) are Langmuir constants related to adsorption capacity and energy of adsorption, respectively. However the data was not in consistence with the Langmuir isotherm model.

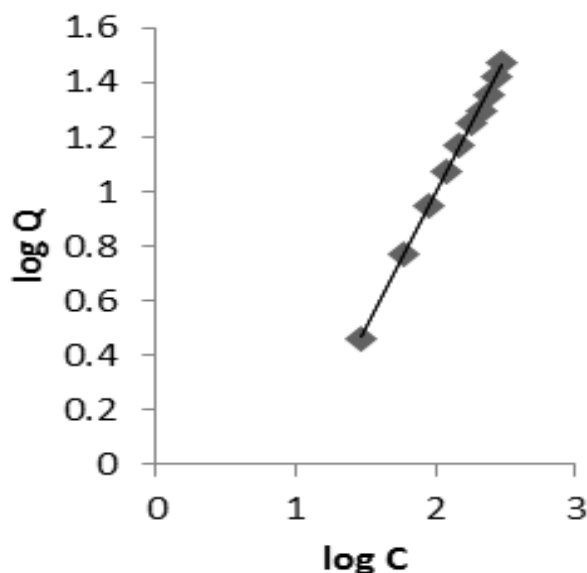


Fig. 7. Equilibrium Freundlich isotherm model for adsorption of Cu(II) on ZnO nanoparticles at pH-5.

Freundlich isotherm model

The Freundlich isotherm is expressed by the following empirical equation [15]:

$$Q = KC^{1/n} \quad (10)$$

The linear form of Freundlich model is expressed as follows:

$$\log Q = \log K + \frac{1}{n} \log C \quad (11)$$

where, Q is the amount of adsorbate sorbed per mass of adsorbent (mg g^{-1}), C is the concentration of the adsorbate (mg l^{-1}), K is characteristic Freundlich constant representing the adsorption capacity (mg g^{-1}) and n is a constant representing adsorption intensity of the system (dimensionless) where $n \ll 1$ indicates that the adsorbate was unfavorably adsorbed on the adsorbent and $1 < n < 10$ indicates that the adsorption was favorable. The linear plot between $\log Q$ versus $\log C$ gives a slope which is equal to the value of $1/n$ and the intercept is $\log K$ as shown in Fig. 7. The value of K comes out to be $0.098 \text{ (mg g}^{-1}\text{)}$ and that of n comes out to be 1.002 . The experimental sorption data was fitted well by the Freundlich isotherm model indicating the heterogeneous nature of the surface sites involved in the process of adsorption. The relatively high correlation coefficient R^2 (0.999) indicates that the experimental data agrees well with the Freundlich adsorption isotherm model [16].

Kinetic modeling

A study of kinetics of adsorption is desirable as it provides information about the mechanism of adsorption. The kinetics of Cu(II) adsorption onto ZnO nanoparticles was evaluated using different models such as pseudo-first-order, pseudo-second-order and intra-particle diffusion models.

Pseudo-first-order model

The pseudo-first-order rate by Lagergren has widely been used. The linearized adsorption rate expression of Lagergren is as follows [17]:

$$\log(Q_e - Q) = \log Q_e - \left(\frac{k_1}{2.303}\right) t \quad (12)$$

where, Q_e is the amount of metal ions adsorbed per unit weight of adsorbent at equilibrium i.e. adsorption capacity (mg g^{-1}), Q is the amount of metal ions adsorbed per unit weight of adsorbent (mg g^{-1}) at any time t and k_1 is the rate constant of first order adsorption in min^{-1} . The value of k_1 has been calculated from the slope of the linear plot of $\log(Q_e - Q)$ versus t which came out to be 0.149 min^{-1} . The first order equation of Lagergren did not apply well throughout the whole contact time which is noticeable from the correlation coefficient R^2 value which comes out to be 0.946 .

Pseudo-second-order model

Pseudo-second-order rate model can be represented in the following form [18]:

$$\frac{t}{Q} = \frac{1}{k_2 Q_e^2} + \left(\frac{1}{Q_e} \right) t \quad (13)$$

where Q_e is the amount of metal ions adsorbed per unit weight of adsorbent at equilibrium i.e., adsorption capacity (mg/g), Q is the amount of adsorbed (mg/g) at any time t and k_2 is rate constant of second order adsorption in $\text{g mg}^{-1} \text{min}^{-1}$.

The plot of t/Q versus t is a straight line as shown in Fig. 8 (a). The k_2 and Q values determined from the slope and intercept of the plot respectively. The correlation coefficient for the second-order kinetics model is 0.99, indicating the applicability of this kinetic equation and the second-order nature of adsorption process of Cu(II) ions onto ZnO nanoparticles. The value of k_2 as determined from the plot of t/Q versus t is $6.707 \times 10^{-2} \text{ g mg}^{-1} \text{min}^{-1}$.

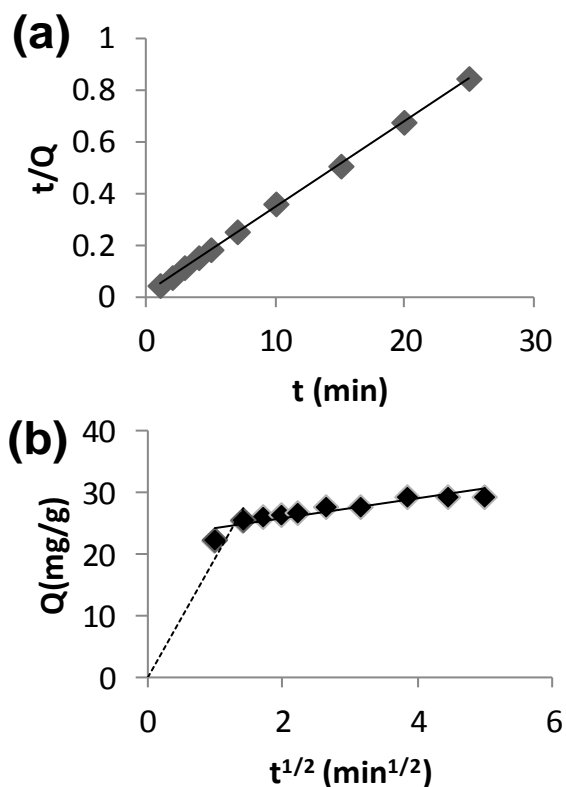


Fig. 8. Kinetic models for adsorption of Cu(II) on ZnO nanoparticles at pH-5, conc.=300 mg/l, amount of adsorbent= 100 mg (a) Pseudo-second-order plot (b) Intra-particle diffusion model.

Intra-particle diffusion model

The kinetics of the adsorption process by intra-particle diffusion model was also evaluated. The adsorbate species are most likely transported from the bulk of the solution

into the solid phase through an intra-particle diffusion process, which often is the rate limiting step in many adsorption processes. The intra-particle diffusion is described by the Weber and Morris diffusion model in the form of eq.14 [19 ,20].

$$Q = K_{id} t^{1/2} + C \quad (14)$$

where, Q is adsorption capacity at any time t (mg g^{-1}), and k_{id} is the intra-particle diffusion rate constant ($\text{mg g}^{-1} \text{min}^{-1/2}$) and C is the intercept (mg g^{-1}). The intra-particle diffusion curve (Fig. 8(b)), shows an initial slope with a dotted line that can be attributed to the faster mass transfer through the boundary layer and/or adsorption on the solid surface, followed by a slow diffusion inside the particles. The intercept C in the equation of Weber and Morris model, is an extrapolation of its second linear 'diffusion' part to the ordinate (solid line in Fig. 8(b)). The lower slope shown by the solid line corresponds to a slower adsorption process. The plot should pass through the origin if the intra-particle diffusion was the only rate controlling step. However, the plot does not pass through the origin, indicating that intra-particle diffusion is involved in the process but is not the only rate limiting mechanism, and some other mechanisms also appear to play an important role. The value of k_{id} , as obtained from the slope, was found to be $1.555 \text{ mg g}^{-1} \text{min}^{-1/2}$. The deviation of the curve from the origin indicates that the processes, surface adsorption and intra-particle diffusion, are both likely to affect the kinetics of adsorbate-adsorbent interaction.

Conclusion

Zinc oxide nanoparticles have been synthesized by the reported method and the characterization carried out by XRD, TEM and DLS indicates the purity of ZnO nanoparticles. The ZnO nanoparticles can be used as a potential adsorbent for Cu(II) ions from aqueous solutions as removal to the extent of 98.71% could be attained. Adsorption of the metal ion was dependent on initial metal ion concentration, contact time, pH and the amount of adsorbent. The pH for maximum adsorption was found to be 5.

Adsorption isotherm studies indicate that the data fits well to the Freundlich isotherm model. The n value indicates that the adsorption process is favoured. Kinetic studies show that the process follows a pseudo-second-order model. Intra-particle diffusion study indicates that in addition to surface adsorption, intraparticle diffusion also occurs but is not the rate determining step.

Acknowledgements

The present work was supported by Technical Education Quality Improvement Programme (TEQIP-II) as M.E. scholarship to one of the authors (Karuna Nalwa) during her ME programme at Dr SSBUCET, Panajb University, Chandigarh, India. Thanks to all scientists referenced throughout the paper whose valuable work has guided the way through to this research work.

References

1. Klabunde, K.J.; Richards, R.M. (Eds.); Nanoscale materials in Chemistry; John Wiley and Sons, New York, **2001**.
DOI: [10.1002/0471220620.ch1](https://doi.org/10.1002/0471220620.ch1)
2. Liu, X.; Hu, Q.; Fang, Z.; Zhang, X.; Zhang, B.; Langmuir, **2009**, 25, 3.
DOI: [10.1021/la802754t](https://doi.org/10.1021/la802754t)
3. WHO, Guidelines for drinking-water quality, fourth edition.
4. Mamalis, A.G.; J.Mater. Process.Technol.,**2007**, 181, 52.
DOI: [10.1016/j.jmatprotec.2006.03.052](https://doi.org/10.1016/j.jmatprotec.2006.03.052)
5. Shao, L.; Chen, J.; China Particuol.,**2005**, 3, 134.
DOI: [10.1016/S1672-2515\(07\)60180-8](https://doi.org/10.1016/S1672-2515(07)60180-8)
6. Khaleel, A.; Kapoor, P.N.; Klabunde, K.J.; Nanostruct. Mater.,**1999**, 11, 459.
DOI: [10.1016/S0965-9773\(99\)00329-3](https://doi.org/10.1016/S0965-9773(99)00329-3)
7. Lin, M.; Zhao, Y.; Wang, S.; Liu, M.; Duan, Z.; Chen, Y.M.; Li, F.; Xu, F.; Lu, T. J.; Biotechnol.Adv.,**2012**, 30, 1551.
DOI: [10.1016/j.biotechadv.2012.04.009](https://doi.org/10.1016/j.biotechadv.2012.04.009)
8. Mahmoud, A.M.; Ibrahim, F.A.; Shaban, S.A.; Youssef, N.A.; Egypt. J. Pet.; 2015, 24, 27.
DOI: [10.1016/j.epje.2015.02.003](https://doi.org/10.1016/j.epje.2015.02.003)
9. Netaji, K.; Rezvani, Z.; Pakizevand, R.; Int. Nano Lett.,**2011**, 1,75.
10. Mehlig, J.P.; Ind. Eng. Chem., Anal. Ed., **1941**, 13, 533.
DOI: [10.1021/i560096a006](https://doi.org/10.1021/i560096a006)
11. Aneesh, P.M.; Vanaja, K.A.; Jayaraj, M.K.; Proc. SPIE, **2007**, 6639,1.
DOI: [10.1117/12.730364](https://doi.org/10.1117/12.730364)
12. Sheela, T.; Nayaka, Y.A.; Viswanatha, R.; Basavanna, S.; Venkatesha, T.G.; Powder Technol.,**2012**, 217, 163.
DOI: [10.1016/j.powtec.2011.10.023](https://doi.org/10.1016/j.powtec.2011.10.023)
13. Kadirvelu, K.; Goel, J.; Rajagopal, C.; J. Hazard. Mater.,**2008**, 153, 502.
DOI: [10.1016/j.jhazmat.2007.08.082](https://doi.org/10.1016/j.jhazmat.2007.08.082)
14. Farah, J.Y.; El-Gendy, N.; Farahat, L.A.;J. Hazard. Mater.,**2007**, 148, 402.
DOI: [10.1016/j.jhazmat.2007.02.053](https://doi.org/10.1016/j.jhazmat.2007.02.053)
15. Jain, C.K.; Hydrol. Sci. J., **2001**, 46, 419.
DOI: [10.1080/02626660109492836](https://doi.org/10.1080/02626660109492836)
16. Bulut, Y.; Tez, Z.; J. Environ. Sci.,**2007**, 19, 160.
DOI: [10.1016/S1001-0742\(07\)60026-6](https://doi.org/10.1016/S1001-0742(07)60026-6)
17. Bulut, Y.; Aydin, H.; Desalination, **2006**, 194, 259.
DOI: [10.1016/j.desal.2005.10.032](https://doi.org/10.1016/j.desal.2005.10.032)
18. Mckay, G.; Ho, Y.S.; Process Biochem.,**1999**, 34, 451.
DOI: [10.1016/S0032-9592\(98\)00112-5](https://doi.org/10.1016/S0032-9592(98)00112-5)
19. McKay, G.; Otterburn, M.S.; Sweeney, A.G.; Water Res.,**1980**, 14, 15.
DOI: [10.1016/0043-1354\(80\)90037-8](https://doi.org/10.1016/0043-1354(80)90037-8)
20. Goswami, A.; Raul, P.K.; Purkait, M.K.; Chem. Eng. Res. Des.,**2012**, 90, 1387.
DOI: [10.1016/j.cherd.2011.12.006](https://doi.org/10.1016/j.cherd.2011.12.006)